Available online at www.sciencedirect.com
SCIENCE DIRECT
Thermochimica Acta 442 (2006) 25–30
thermochimica acta
www.elsevier.com/locate/tca

Melting and reorganization of the crystalline fraction and relaxation of the rigid amorphous fraction of isotactic polystyrene on fast heating (30,000 K/min)

Alexander A. Minakov [1], Dmitry A. Mordvintsev, Rob Tol [2], Christoph Schick *

University of Rostock, Institute of Physics, Universitä tsplatz 3, 18051 Rostock, Germany

Available online 18 January 2006

Abstract

For polymers the origin of the multiple melting peaks observed in DSC curves is still controversially discussed. This is due to the difficulty to investigate the melting of the originally formed crystals exclusively. Recrystallization is a fast process and most experimental techniques applied so far do not allow fast heating in order to prevent recrystallization totally. Developments in thin-film (chip) calorimetry allow scanning rates as high as several thousand Kelvin per second. We utilized a chip calorimeter based on a commercially available vacuum gauge, which is operated under non-adiabatic conditions. The calorimeter was used to study the melting of isothermally crystallized isotactic polystyrene (iPS). Our results on melting at rates up to 30,000 K/min (500 K/s) give evidence for the validity of a melting–recrystallization–remelting process for iPS at low scanning rates (DSC). At isothermal conditions iPS forms crystals, which all melt within a few dozens of K slightly above the isothermal crystallization temperature. There is no evidence for the formation of multimodal populations of crystals with significantly different stability (melting temperatures). Furthermore, relaxation (devitrification) of the rigid amorphous fraction occurs in parallel to melting. Superheating of the crystals is of the order of 25 K at 30,000 K/min.

Keywords: Polymer crystallization; Multiple melting; Rigid amorphous; Fast calorimetry; iPS

1. Introduction

A lamellar stack model describes the morphology of most semicrystalline polymers reasonable well. Although this morphology feature was discovered already 65 years ago [1] the question how polymer crystals are formed is still under debate, see e.g. [2–6] and references therein. It is the chain structure of the polymer molecules, which forces polymers to form morphologies, build up from folded chain lamellae and spherulites. The equilibrium structure – the extended chain crystal – is commonly not realized. Consequently these structures are not in thermodynamic equilibrium. The deviation from equilibrium causes significant reorganization and recrystallization already at crystallization or at annealing and heating. Reorganization at heating of isotactic polystyrene (iPS) was, as an example, extensively studied by Strobl et al. [7,8] applying X-ray diffraction. This makes description of polymer melting a very complex task. Crystallization at large super cooling yields structures, which are especially far from thermodynamic equilibrium. Melting–recrystallization[3]–remelting sequences are often considered to describe the complex melting behaviour observed. Calorimetry and especially differential scanning calorimetry (DSC) at rates of the order of 10 K/min is commonly applied to study polymer melting. Other techniques like temperature dependent X-ray diffraction, e.g. [7,8], transmission electron microscopy [9] or in situ atomic force microscopy (AFM), e.g. [10–13], are used to study polymer melting too and partly support the idea of melting–recrystallization. But other models like the creation of secondary lamella, the existence of bimodal crystal stabilities as discussed by Petermann et al. [9] or the

* Corresponding author. Tel.: +49 381 498 6880; fax: +49 381 498 6882.
E-mail address: christoph.schick@uni-rostock.de (C. Schick).
[1] On leave from the Natural Science Research Centre of A.M. Prokhorov General Physics Institute of Russian Academy of Science, Vavilov Street 38, 119991 Moscow, Russia.
[2] On leave from SciTe, Ridder Vosstraat 6, 6162 AX Geleen, The Netherlands, within a European Union funded grant from COST P12.

[3] Recrystallization is used in a very broad meaning here. It covers all processes leading to a slightly more stable lamellae or part of single lamellae including annealing.

0040-6031/$ – see front matter © 2005 Elsevier B.V. All rights reserved.
doi:10.1016/j.tca.2005.11.032

relaxation of the rigid amorphous fraction are considered too to describe the multiple peaks occurring in DSC curves [14–17]. In a recent paper Cebe et al. [18] report a detailed study on the crystal melting and relaxation of the rigid amorphous fraction in iPS using temperature modulated DSC (TMDSC). The main conclusion drawn was that for iPS the observed three peaks can be explained by dual reversible crystal melting and irreversible enthalpic relaxation of the rigid amorphous fraction (RAF).

In a previous study [19] we were able to show that poly(ethylene terephthalate) (PET) forms a monomodale distribution of crystallite sizes or crystal stabilities on isothermal crystallization. At heating with 162,000 K/min (2700 K/s) only a single melting peak is observed for samples isothermally crystallized in the broad temperature range between 114 and 230 °C. No separate devitrification of the rigid amorphous fraction of PET was observed at such high rates.

These studies became possible because of recent developments in fast scanning calorimetry. Pijpers et al. extended the heating and cooling rate range of DSC to rates as high as 500 K/min (HyperDSC™) [20]. Developments in thin-film (chip) calorimetry [21–23] allow even much higher rates also for low thermal conducting polymer samples as shown by Allen et al. [24–26]. We have developed a chip calorimeter in order to study polymeric samples at fast scanning [19,27–30]. The calorimeter is based on a commercially available vacuum gauge TCG 3880 from Xensor Integration, Nl, [31] and allows measurements at rates up to 600,000 K/min (10,000 K/s). In the present study it was applied to the melting of isothermally crystallized iPS in order to see if a double melting endotherm or a separate relaxation of the rigid amorphous fraction under conditions when recrystallization is suppressed can be detected.

2. Experimental

DSC and Hyper DSC™ measurements were performed utilizing a Perkin-Elmer Pyris Diamond DSC equipped with an Intracooler II and nitrogen purge. The instrument was calibrated by indium and zinc for temperature at the scanning rate of interest and by sapphire for heat flow. The sample (1 or 5 mg, depending on heating rate) was wrapped in aluminium foil of a few milligrams only to minimize thermal lag [20].

Fast scanning experiments were performed applying a chip calorimeter based on the thermal conductivity gauge TCG-3880 [31] as shown in Fig. 1. The gauge consists of a 0.5 μm Si_3N_x membrane with a thin-film thermopile and a resistive film-heater placed at the center of the membrane. All electrical connections are covered by an additional 0.7 μm SiO_2 layer for electrical isolation and protection. The six hot junctions of a semi conducting thermopile – the white spots around the central region in the photograph – are placed around the heated area, ca. 50 μm × 100 μm. The cold junctions are placed at the silicon frame fixing the membrane, ca. 1 mm from the center. Thus the cold-junction temperature equals the temperature of the holder, which is close to the temperature of the thermostat. The measurements are performed in an ambient gas atmosphere rather than under adiabatic conditions. Therefore measurements on controlled cooling are possible too. The calorimeter allows measurements at rates up to 600,000 K/min (10,000 K/s). A more detailed description of the calorimeter, the measurement algorithm, and calibration can be found elsewhere [19,27,28].

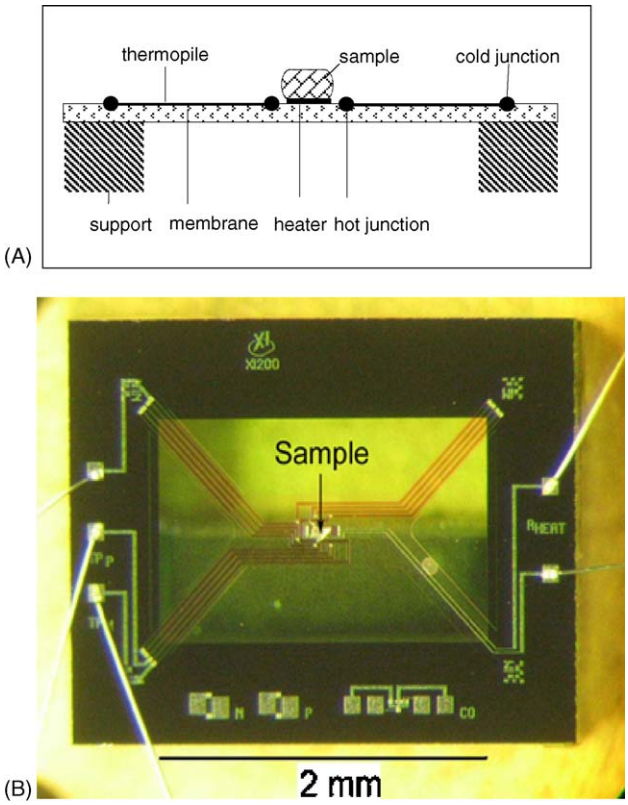

Fig. 1. Thin-film chip calorimeter based on the thermal conductivity gauge TCG-3880. Scheme (A) and microphotograph of the frame and the membrane loaded with a sample (B).

Isotactic (90%) polystyrene powder with a weight-average molecular weight of 400,000 g/mol was obtained from Scientific Polymer Products Inc. This is the same polymer as studied by Cebe et al. [18] or Strobl et al. [7,8]. From the powder a tiny peace of the order of a few hundred nanograms was transferred on the sensor. The sample was moved on top of the heater of the calorimetric sensor, see Fig. 1. To avoid damaging of the sensor membrane (ca. 500 nm thick) the sample was transferred to and moved on the membrane using a soft cooper wire (diameter 50 μm). A stereomicroscope was used to control the movement. When the sample was on the right place an electrical current through the heater was switched on to melt the sample for the first time. This way the sample was fixed at a position just on top of the heater. Because of strong adhesive forces the sample-membrane thermal contact was good and very stable after a few heating-cooling cycles, which is important for calorimetric measurements [32,33].

The crystallization conditions were chosen as described in [18]. The iPS sample was crystallized at 140 and 170 °C for 12 and 4 h, respectively. But here the samples were crystallized from the melt (melt crystallization) while in [18] the sample were first quenched below glass transition temperature (cold crystallization). Because of limitations regarding data collection slow cooling, say 100 K/min, from the melt down below the glass

transition and slow heating to the crystallization temperature (cold crystallization) was not possible with the chip calorimeter. At rates of several thousand Kelvin per minute as commonly used with the chip calorimeter no difference between cold and melt crystallization was seen. Therefore all crystallizations were performed as melt crystallization.

The iPS samples of ca. 5 mg, 1 mg and 400 ng for DSC, HyperDSC and the chip calorimeter, respectively, were molten at 250 °C for a very short time to minimize degradation of the sample. After isothermal crystallization the sample was quenched below glass transition at 30 °C. The quenching rate was 200 and 600,000 K/min (10^4 K/s) for DSC and the chip calorimeter, respectively. Then the measurements were performed at different heating rates.

3. Results

The multiple melting peaks in isothermally crystallized iPS are known since long time, see e.g. [17,34,35]. Fig. 2 shows typical DSC curves at 10 K/min for iPS crystallized at 140 and 170 °C, respectively. At large super cooling (low T_c) a low and a high melting endotherm is observed. At lower super cooling (high T_c) even multiple melting peaks occur.

From the DSC scans in Fig. 2 the fractions according a three-phase model were obtained in the common way from the heat capacity increment at the glass transition and are given in Table 1. The values for the sample crystallized at 140 °C are very comparable to the values published by Cebe at al. [18] and Strobl et al. [7,8]. For the sample crystallized at 170 °C crystallinity

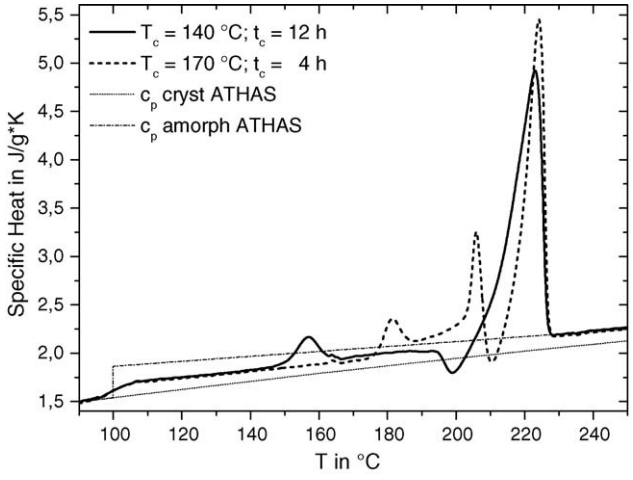

Fig. 2. Temperature dependences of the specific heat capacity of a 4 mg iPS sample at heating rate 10 K/min. The sample was crystallized at T_c = 140 °C, t_c = 12 h (solid line) and T_c = 170 °C, t_c = 4 h (dashed line), and quenched below glass transition. The curves for amorphous and crystalline iPS are shown too [36].

Table 1
Fractions according a three-phase model

T_c (°C)	CRF	MAF	RAF
140	0.32	0.45	0.23
170	0.33	0.5	0.17

is lower compared to [18] but the same as reported in [8] for the same material. This is most probably due to the fact that we used melt crystallization and Cebe et al. [18] performed cold crystallization. At cooling at moderate rates (<100 K/min) it is assumed to form nuclei at cooling to the glass transition, which are missing in case of melt crystallization or much faster quenching. Why our data are in accordance with the data presented in [8], which are for cold crystallized samples, is not understood.

If the high temperature melting peak is only due to recrystallization during the scan it should disappear when recrystallization could be prevented by fast heating, provided at the initial isothermal crystallization a monomodal population of lamellae was formed. In order to clarify this we performed experiments at different heating rates. At high heating rates it should be possible to differentiate between devitrification of the RAF and melting of the originally formed crystals too.

The results from measurements at different heating rates up to 30,000 K/min (500 K/s) for samples melt crystallized at 170 and 140 °C are shown in Fig. 3.

The iPS sample melt crystallized at 170 °C, Fig. 3A, shows a very complex melting behaviour. At the two lowest heating rates three peaks appear at 180, 205 and 220 °C, respectively. The high-temperature melting peak decreases at increasing heating rate. At 500 K/min all three peaks merge to one broad melting peak ranging from 195 to 240 °C. Obviously, there is no direct indication for any multimodal distribution in melting temperatures, etc. for the crystallization temperature of 170 °C. But the observed peak is very broad and probably the superposition of multiple peaks. The crystals formed at 140 °C, Fig. 3B, are less stable. Even at 500 K/min two well separated peaks are seen, indicating recrystallization. But the increasing low temperature peak and the shift of the second melting peak towards lower temperatures at increasing heating rate strongly support the melting–recrystallization–remelting model for this sample too. Obviously, 500 K/min is not fast enough to prevent recrystallization.

In order to increase heating rate even more we used the chip calorimeter described in the experimental part. For both samples only one peak can be seen at heating rates above 6000 K/min (100 K/s). For the sample crystallized at 170 °C the broad peak observed at 500 K/min becomes significantly smaller indicating the occurrence of recrystallization even at 500 K/min. As for PET [19] the first peak (annealing peak) must be considered as part of the melting of the originally formed crystals. For both samples this peak shifts significantly to higher temperatures indicating super-heating.

4. Discussion

From DSC and a chip calorimeter we obtained melting curves for isothermally crystallized iPS for heating rates ranging from 10 to 30,000 K/min (0.17–500 K/s). For iPS crystallized at 170 °C a heating rate of 500 K/min is high enough to prevent most recrystallization during the scan, see Fig. 3A. With increasing super cooling (lower T_c) higher and higher rates are needed to prevent recrystallization during the scan. To illustrate

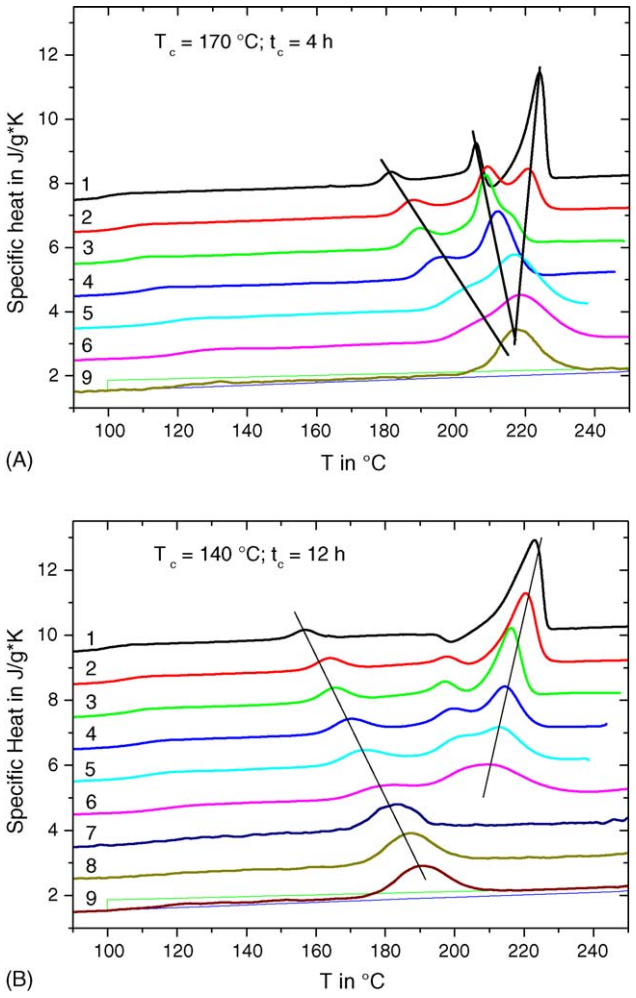

Fig. 3. Temperature dependences of the specific heat capacity of 400 ng–4 mg iPS samples at the following heating rates: 1 – 10 K/min (0.16 K/s) 4 mg, 2 – 50 K/min (0.83 K/s) 4 mg, 3 – 100 K/min (1.6 K/s) 0.5 mg, 4 – 200 K/min (3.3 K/s) 0.5 mg, 5 – 400 K/min (6.6 K/s) 0.5 mg, 6 – 500 K/min (8.3 K/s) 0.5 mg, 7 – 6000 K/min (100 K/s) 400 ng, 8 – 15,000 K/min (250 K/s) 400 ng, 9 – 30,000 K/min (500 K/s) 400 ng. The samples were crystallized at 170 °C (A) and 140 °C (B) for 12 and 4 h, respectively. The curves are vertically shifted and the straight lines are guides to the eyes only.

the behaviour we combined DSC and chip calorimeter results for the samples crystallized at 170 and 140 °C in Fig. 3.

At increasing heating rate for both crystallization temperatures the highest temperature peak is reduced and shifted to lower temperatures while the low temperature peak increases in area and finally takes over the whole melting enthalpy. This observation is just as expected for a melting–recrystallization–remelting model. Our results, covering more than three orders of magnitude in heating rate, show that there is no bimodal distribution in crystal size or crystal stability present in isothermally crystallized iPS. Otherwise one would expect to see a double peaked melting endotherm even at the highest rates. This finding is in agreement with the data obtained from X-ray diffraction by Strobl et al. [7,8] who found no changes in lamellae thickness during isothermal crystallization but a thickening process on subsequent heating.

The peak temperature of the low temperature endotherm depends strongly on heating rate. This is because the peak temperature equals the temperature where the difference between melting and recrystallization rate is maximal. At slightly higher temperatures – when the excess heat flow is close to zero – a balance regarding melting and recrystallization is established. At low rates, as long as a second melting peak is observed, the maximum is not at all related to some maximum in the lamella thickness distribution as considered for the construction of a Hoffman–Weeks plot [37]. See also a detailed discussion by Yamada et al. [38,39]. Very high heating rates are needed to prevent recrystallization during the melting of iPS and to obtain a meaningful melting temperature for the lamellae formed at isothermal crystallization. Under conditions of fast heating super-heating has to be considered too. It is therefore, from a technical point of view alone, very questionable if a Hoffman–Weeks extrapolation can give correct values for the equilibrium melting temperature of iPS.

The sample crystallized at 140 °C shows a complex melting behaviour including an exothermic effect around 200 °C at heating rate 10 K/min. The occurrence of this pronounced effect, which disappears at slightly higher rates as seen in Fig. 3B, can be related to the correspondence of the experimental time scale and that of melting–recrystallization. This points to another interesting question namely the temperature dependence of melting and recrystallization rates. So far we can only say qualitatively that recrystallization rate becomes slower at higher temperature and in the vicinity of the highest endotherm it is much slower than melting.

Having a tool in hand to study the melting of isothermally crystallized iPS without interference of recrystallization allows us to address the question of relaxation of the RAF on heating. If relaxation of the RAF occurs separately from crystal melting one would expect to see a step in heat capacity in the temperature range of relaxation. According Cebe et al. [18] at low heating rates the lowest endotherm should be due to the nonreversing enthalpic relaxation of the RAF. In order to check this hypothesis we compare in Fig. 4 heat capacities at slow and fast heating, 10 and 30,000 K/min, for the iPS sample crystallized at 140 °C.

For both heating rates above glass transition heat capacity follows the line expected from a three-phase model taking into account crystalline, mobile amorphous and rigid amorphous fractions, which are given in Table 1, for details see e.g. [17,18,40]. For the low heating rate after the first endothermic peak heat capacity coincides with that expected according a two-phase model taking into account crystalline and mobile amorphous fractions only as already shown by Cebe et al. [18]. If the first endothermic peak is caused by an enthalpic relaxation of the RAF one would expect to see a similar effect or at least some step in the heat capacity curve at temperatures around 160 °C for the fast heating too. But there is nothing to see at fast heating. Heat capacity reaches the liquid line above the single melting peak. This indicates that melting of crystals and relaxation of the RAF occurs in the temperature range of the broad single melting peak, most probably simultaneously. It should be mentioned here that accuracy of heat of fusion measurement is not as good as for heat capacity outside the melting region at

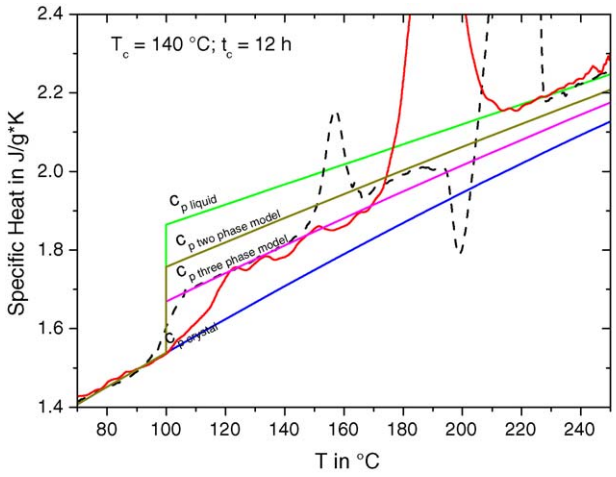

Fig. 4. Heat capacity of iPS sample crystallized at 140 °C for 12 h at heating rate 10 K/min (dashed line) and 30,000 K/min (solid line). Expected heat capacities [36] for the liquid, the crystalline and the semicrystalline iPS according a two- and three-phase model, see Table 1 are shown too.

fast scanning. From the fast scanning we obtain crystallinity of 0.2 and consequently a rigid amorphous fraction of 0.35. Actually we do not know if this is real or an experimental artifact. But in any case there is a solid fraction of about 0.55 as for the slowly heated sample, which is indicated by the three-phase line in Fig. 4.

At fast heating we see a significant shift of the glass transition to higher temperatures. The T_g of the mobile amorphous fraction shifts from 100 °C at 10 K/min to about 115 °C in accordance with previous data on rate dependence of glass transition [41]. If we consider the same apparent activation energy for the relaxation of the RAF the beginning of the heat capacity increase (peak or step) should be shifted to 160 °C. But on fast heating nothing special happens around 160 °C. It is therefore unlikely that the annealing peak is related to the nonreversing enthalpic relaxation of the RAF only.

But why do we see the step in heat capacity at the low temperature endotherm at slow heating? As shown for polycarbonate and polyhydroxybuterate [40] and by Cebe et al. for iPS [18] heat capacity changes from the value expected from a three-phase model to that according a two-phase model in the temperature range of the low temperature endotherm. Combining these earlier observations with a continuous melting–recrystallization–remelting model, which is supported by the results obtained by Strobl et al. [7,8] too and the fast heating experiments, one can discuss the observations as follows. At low heating rates melting of the crystals starts at the rising flank of the lowest temperature endotherm. Parallel to crystal melting the RAF surrounding the just molten crystals relaxes. As shown in [19,29] the melt is than in a state (conformation) allowing very rapid (within milliseconds) recrystallization. This recrystallization creates more stable crystals but does not significantly increase crystallinity. Assuming a continuous melting–recrystallization–remelting the remaining amorphous material in between the crystals may not be vitrified as in the case of slow isothermal crystallization [18,40]. If the amorphous material does not vitrify heat capacity should be the same as expected from a two-phase model as soon as the continuous melting–recrystallization–remelting starts and that seems to be what we observe. Why the amorphous material does not vitrify we can only speculate. May be there are not enough stable crystals present (they may melt continuously). Or there is not enough time to vitrify the amorphous material before the crystals melt again. From our study on polycarbonate [40] we have seen that after annealing above the first endotherm the RAF is reestablished after some time. If the rigid amorphous fraction would be reestablished immediately continues melting–recrystallization would not be possible because the presence of RAF would prevent crystallization at that spot. From Strobl's X-ray experiments [7,8] we know additionally that not only crystal thickness but also long spacing increases. This indicates that melting–recrystallization is not a local process related to single lamellae. There must be something happen on length scales comparable to the lamellae stack, which is much larger than the thickness of single lamellae.

5. Conclusion

Fast scanning calorimetry utilizing a thin film vacuum gauge as calorimeter in combination with DSC covers a scanning rate range between 6×10^{-3} and 6×10^{5} K/min (10^{-4} and 10^{4} K/s). These eight orders of magnitude allow studying the kinetics of different processes. Our results on melting at rates up to 30,000 K/min (500 K/s) support the validity of a melting–recrystallization–remelting process for iPS at low scanning rates (DSC). The iPS forms crystals at isothermal melt crystallization, which all melt within a few dozens of K slightly above the isothermal crystallization temperature. There is no evidence for the formation of multimodal distributions of crystals with different stability (melting temperatures) at isothermal crystallization of iPS. The single broad melting peaks at high heating rates show that broad monomodal distributions of lamellae thicknesses exist. Superheating of the crystals is of the order of 25 K at 500 K/s. No evidence was found supporting a separate relaxation of the RAF. The observed changes of heat capacity at the lowest endotherm at slow heating can be explained by continuous melting–recrystallization–remelting assuming no vitrification of the amorphous material on continuous heating. This assumption is justified because recrystallization needs mobility in the melt which surrounds the recrystallizing volume. In iPS the RAF relaxes simultaneously with crystal melting. The crystals created at the isothermal crystallization temperature melt at temperatures close to the first endotherm. Therefore the RAF relaxes at that temperature too. That no changes in crystallinity are observed at the lowest endotherm does not contradict the melting–recrystallization–remelting model because recrystallization occurs on a millisecond time scale [19,29] and can not be resolved with conventional experiments like DSC, IR spectroscopy or X-ray scattering at slow heating rates of the order of Kelvin per minute.

Acknowledgements

This work was financially supported by the German Science Foundation (DFG) Grants Schi 331/7, 436 RUS 17/49/03 and Perkin-Elmer. Rob Tol is indebted to the European Community for funding a STSM within COST Action P12. Christoph Schick acknowledges valuable discussions with P. Cebe, Medford, MA, USA and G. Strobl, Freiburg, Germany.

References

[1] K.H. Storks, J. Am. Chem. Soc. 60 (1938) 1753–1761.
[2] G. Strobl, Eur. Phys. J. E3 (2000) 165–183.
[3] B. Lotz, Eur. Phys. J. E3 (2000) 185–194.
[4] S.Z.D. Cheng, C.Y. Li, L. Zhu, Eur. Phys. J. E3 (2000) 195–197.
[5] M. Muthukumar, Eur. Phys. J. E3 (2000) 199–202.
[6] J.U. Sommer, G. Reiter, Polymer Crystallization – Obervations Concepts and Interpretations, Springer-Verlag, Berlin, Heidelberg, NewYork, Barcelona, HongKong, London, Milan Paris, Singapore, Tokyo, 2002.
[7] M. Al-Hussein, G. Strobl, Eur. Phys. J. E6 (2001) 305–314.
[8] M. Al-Hussein, G. Strobl, Macromolecules 35 (2002) 1672–1676.
[9] T. Liu, S. Yan, M. Bonnet, I. Lieberwirth, K.-D. Rogausch, J. Petermann, J. Mater. Sci. 35 (2000) 5047–5055.
[10] L.G.M. Beekmans, D.W. van der Meer, G.J. Vancso, Polymer 43 (2002) 1887–1895.
[11] D.A. Ivanov, Z. Amalou, S.N. Magonov, Macromolecules 34 (2001) 8944–8952.
[12] L.G.M. Beekmans, G.J. Vancso, Polymer 41 (2000) 8975–8981.
[13] Y. Jiang, D.D. Yan, X. Gao, C.C. Han, X.G. Jin, L. Li, Y. Wang, C.M. Chan, Macromolecules 36 (2003) 3652–3655.
[14] S. Sohn, A. Alizadeh, H. Marand, Polymer 41 (2000) 8879–8886.
[15] B.B. Sauer, W.G. Kampert, E.N. Blanchard, S.A. Threefoot, B.S. Hsiao, Polymer 41 (2000) 1099–1108.
[16] Z.G. Wang, B.S. Hsiao, B.B. Sauer, W.G. Kampert, Polymer 40 (1999) 4615–4627.
[17] H. Xu, B.S. Ince, P. Cebe, J. Polym. Sci. Part B 41 (2003) 3026–3036.
[18] H. Xu, P. Cebe, Macromolecules 37 (2004) 2797–2806.
[19] A.A. Minakov, D.A. Mordvintsev, C. Schick, Polymer 45 (2004) 3755.
[20] M.F.J. Pijpers, V.B.F. Mathot, B. Goderis, R. Scherrenberg, E. van der Vegte, Macromolecules 35 (2002) 3601–3613.
[21] D.W. Denlinger, E.N. Abarra, K. Allen, P.W. Rooney, M.T. Messer, S.K. Watson, F. Hellman, Rev. Sci. Instrum. 65 (1994) 946–958.
[22] S.L. Lai, G. Ramanath, L.H. Allen, P. Infante, Z. Ma, Appl. Phys. Lett. 67 (1995) 1229–1231.
[23] M. Merzlyakov, Thermochim. Acta, this issue.
[24] M.Y. Efremov, J.T. Warren, E.A. Olson, M. Zhang, A.T. Kwan, L.H. Allen, Macromolecules 35 (2002) 1481–1483.
[25] M.Y. Efremov, E.A. Olson, M. Zhang, L.H. Allen, Thermochim. Acta 403 (2003) 37–41.
[26] M.Y. Efremov, E.A. Olson, M. Zhang, Z. Zhang, L.H. Allen, Phys. Rev. Lett. 91 (2003) 85703-1-4.
[27] S.A. Adamovsky, A.A. Minakov, C. Schick, Thermochim. Acta 403 (2003) 55–63.
[28] S.A. Adamovsky, C. Schick, Thermochim. Acta 415 (2004) 1–7.
[29] A.A. Minakov, D.A. Mordvintsev, C. Schick, Faraday Discuss. 128 (2005) 261–270.
[30] A.A. Minakov, S.A. Adamovsky, C. Schick, Thermochim. Acta 432 (2005) 177–185.
[31] http://www.xensor.nl/.
[32] I. Hatta, A.A. Minakov, Thermochim. Acta 330 (1999) 39–44.
[33] A.A. Minakov, Thermochim. Acta 345 (2000) 3–12.
[34] P.J. Lemstra, T. Kooistra, G. Challa, J. Polym. Sci. Part A-2: Polym. Phys. 10 (5) (1972) 823–833.
[35] J. Boon, G. Challa, D.W. van Krevelen, J. Polym. Sci. Part A-2: Polym. Phys. 6 (10) (1968) 1791–1801.
[36] B. Wunderlich, Pure Appl. Chem. 67 (1995) 1019–1026, http://web.utk.edu/athas/.
[37] J.D. Hoffman, J.J. Weeks, J. Res. Natl. Bur. Stand. A: Phys. Chem. 66 (1962) 13–28.
[38] K. Yamada, M. Hikosaka, A. Toda, S. Yamazaki, K. Tagashira, Macromolecules 36 (2003) 4790–4801.
[39] K. Yamada, M. Hikosaka, A. Toda, S. Yamazaki, K. Tagashira, Macromolecules 36 (2003) 4802–4812.
[40] C. Schick, A. Wurm, A. Mohammed, Colloid Polym. Sci. 279 (2001) 800–806.
[41] C. Schick, A. Hensel, J. Non-Cryst. Solids 235–237 (1998) 510–516.